Nonlocal spin-sensitive electron transport in diffusive proximity heterostructures

Mikhail S. Kalenkov
I.E. Tamm Department of Theoretical Physics, P.N. Lebedev Physics Institute, 119991 Moscow, Russia

Andrei D. Zaikin
Institute of Nanotechnology, Karlsruhe Institute of Technology (KIT), 76021 Karlsruhe, Germany and I.E. Tamm Department of Theoretical Physics, P.N. Lebedev Physics Institute, 119991 Moscow, Russia
(Received 19 May 2010; published 28 July 2010)

We formulate a quantitative theory of nonlocal electron transport in three-terminal disordered ferromagnet-superconductor-ferromagnet (FSF) structures. We demonstrate that magnetic effects have different implications. While strong exchange field suppresses disorder-induced electron interference in ferromagnetic electrodes, spin-sensitive electron scattering at superconductor-ferromagnet interfaces can drive the total nonlocal conductance g_{12} negative at sufficiently low energies. At higher energies, magnetic effects become less important and the nonlocal resistance behaves similarly to the nonmagnetic case. Our predictions can be directly tested in future experiments on nonlocal electron transport in hybrid FSF structures.

DOI: 10.1103/PhysRevB.82.024522 PACS number(s): 74.45.+c, 72.25.Ba, 73.23.−b, 74.78.Na

I. INTRODUCTION

The phenomenon of Andreev reflection (AR) (Ref. 1) is well known to be responsible for transport of subgap electrons across an interface between a normal metal (N) and a superconductor (S). While this phenomenon is essentially local in hybrid proximity structures with only one NS interface, the situation in multiterminal devices with two or more NS interfaces (such as, e.g., NSN structures) can be more complicated because in addition to local AR electrons can suffer nonlocal or crossed AR (CAR).[2] This phenomenon of CAR enables direct experimental demonstration of entanglement between electrons in spatially separated N electrodes and can strongly influence nonlocal transport of electrons in hybrid NSN systems.[3,4]

Nonlocal electron transport in the presence of CAR was recently investigated both experimentally[5–10] and theoretically[3,4,11–19] demonstrating a rich variety of physical processes involved in the problem. For instance, the effect of CAR on the subgap nonlocal conductance of NSN structures is exactly compensated by elastic cotunneling (EC) provided only the lowest order terms in NS interface transmissions are accounted for.[3] Taking into account higher order processes in barrier transmissions eliminate this feature and yield nonzero values of cross-conductance.[4] One can also expect that interactions[11] or external ac bias[12] can lift the cancellation between EC and CAR contributions already in the lowest order in barrier transmissions.

Another nontrivial issue is the effect of disorder. Theoretical analysis of CAR in different disordered NSN structures was carried out in Refs. 13–17. In particular, it was demonstrated[17] that an interplay between CAR, quantum interference of electrons, and nonlocal charge imbalance dominates the behavior of diffusive NSN systems being essential for quantitative interpretation of a number of experimental observations.[7–9]

Yet another important property of both local and nonlocal Andreev reflection processes is that they essentially depend on spins of scattered electrons. Hence, CAR should be sensitive to magnetic properties of normal electrodes. This sensitivity was indeed demonstrated already in the first experiments on ferromagnet-superconductor-ferromagnet (FSF) structures[5] where the dependence of nonlocal conductance on the polarization of ferromagnetic terminals was found. Theoretical analysis of spin-resolved CAR was carried out in Ref. 3 in the lowest order in tunneling and in Refs. 18 and 19 to all orders in the interface transmissions. This analysis revealed a number of nontrivial features of nonlocal spin-dependent electron transport which can be tested in future experiments.

Note that previous work[3,18,19] merely concentrated on ballistic electrodes whereas in realistic experiments one usually deals with diffusive hybrid FSF structures. Therefore it is highly desirable to formulate a theory which would adequately describe an interplay between disorder and spin-resolved CAR. This is the main goal of the present paper. The structure of our paper is as follows. In Sec. II we will formulate our model and outline our basic formalism of quasiclassical Green's functions. This formalism will be employed in Sec. III where we present the solution of Usadel equations and derive general expressions for the nonlocal spin-dependent conductance and resistance for diffusive three-terminal FSF structures at different directions of interface magnetizations. Concluding remarks are presented in Sec. IV of our paper.

II. MODEL AND BASIC FORMALISM

Let us consider a three-terminal diffusive FSF structure schematically shown in Fig. 1. Two ferromagnetic terminals F_1 and F_2 with resistances r_{N_1} and r_{N_2} and electric potentials V_1 and V_2 are connected to a superconducting electrode of length L with normal-state (Drude) resistance r_L and electric potential $V=0$ via tunnel barriers. The magnitude of the exchange field $h_{1,2}=|\boldsymbol{h}_{1,2}|$ in both ferromagnets F_1 and F_2 is assumed to be much bigger than the superconducting order parameter Δ of the S terminal and, on the other hand, much smaller that the Fermi energy, i.e., $\Delta \ll h_{1,2} \ll \epsilon_F$.

 ©2010 The American Physical Society

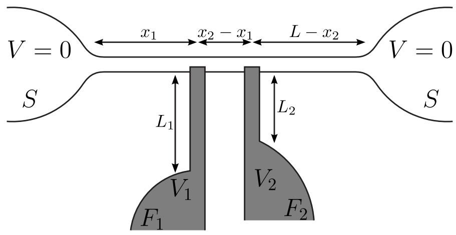

FIG. 1. FSF structure under consideration.

The latter condition allows to perform the analysis of our FSF system within the quasiclassical formalism of Usadel equations for the Green-Keldysh matrix functions G. In each of our metallic terminals these equations can be written in the form[20]

$$iD\,\nabla(\check{G}\,\nabla\,\check{G}) = [\check{\Omega} + eV, \check{G}], \quad \check{G}^2 = 1, \tag{1}$$

where D is the diffusion constant, V is the electric potential, $\check{G}$ and $\check{\Omega}$ are 8×8 matrices in Keldysh-Nambu-spin space (denoted by check symbol)

$$\check{G} = \begin{pmatrix} \check{G}^R & \check{G}^K \\ 0 & \check{G}^A \end{pmatrix}, \quad \check{\Omega} = \begin{pmatrix} \check{\Omega}^R & 0 \\ 0 & \check{\Omega}^A \end{pmatrix}, \tag{2}$$

$$\check{\Omega}^R = \check{\Omega}^A = \begin{pmatrix} \varepsilon - \hat{\boldsymbol{\sigma}}\boldsymbol{h} & \Delta \\ -\Delta^* & -\varepsilon + \hat{\boldsymbol{\sigma}}\boldsymbol{h} \end{pmatrix}, \tag{3}$$

where ε is the quasiparticle energy, $\Delta(T)$ is the superconducting order parameter which will be considered real in a superconductor and zero in both ferromagnets, $\boldsymbol{h} \equiv \boldsymbol{h}_{1(2)}$ in the first (second) ferromagnetic terminal, $\boldsymbol{h} \equiv 0$ outside these terminals, and $\hat{\boldsymbol{\sigma}} = (\hat{\sigma}_1, \hat{\sigma}_2, \hat{\sigma}_3)$ are Pauli matrices in spin space.

Retarded and advanced Green's functions $\check{G}^R$ and $\check{G}^A$ have the following matrix structure:

$$\check{G}^{R,A} = \begin{pmatrix} \hat{G}^{R,A} & \hat{F}^{R,A} \\ -\hat{F}^{R,A} & -\hat{G}^{R,A} \end{pmatrix}. \tag{4}$$

Here and below 2×2 matrices in spin space are denoted by hat symbol.

Having obtained the expressions for the Green-Keldysh functions $\check{G}$ one can easily evaluate the current density $\boldsymbol{j}$ in our system with the aid of the standard relation

$$\boldsymbol{j} = -\frac{\sigma}{16e}\int Sp[\tau_3(\check{G}\,\nabla\,\check{G})^K]d\varepsilon, \tag{5}$$

where σ is the Drude conductivity of the corresponding metal and τ_3 is the Pauli matrix in Nambu space.

In what follows it will be convenient for us to employ the so-called Larkin-Ovchinnikov parameterization of the Keldysh Green's function

$$\check{G}^K = \check{G}^R\check{f} - \check{f}\check{G}^A, \quad \check{f} = \hat{f}_L + \tau_3\hat{f}_T, \tag{6}$$

where the distribution functions $\hat{f}_L$ and $\hat{f}_T$ are 2×2 matrices in the spin space.

For the sake of simplicity we will assume that magnetizations of both ferromagnets and the interfaces (see below) are collinear. Within this approximation the Green's functions and the matrix $\check{\Omega}$ are diagonal in the spin space and the diffusionlike equations for the distribution function matrices $\hat{f}_L$ and $\hat{f}_T$ take the form

$$-D\,\nabla\,[\hat{D}^T(\boldsymbol{r},\varepsilon)\,\nabla\,\hat{f}_T(\boldsymbol{r},\varepsilon)] + 2\hat{\Sigma}(\boldsymbol{r},\varepsilon)\hat{f}_T(\boldsymbol{r},\varepsilon) = 0, \tag{7}$$

$$-D\,\nabla\,[\hat{D}^L(\boldsymbol{r},\varepsilon)\,\nabla\,\hat{f}_L(\boldsymbol{r},\varepsilon)] = 0, \tag{8}$$

where

$$\hat{\Sigma}(\boldsymbol{r},\varepsilon) = -i\Delta\ \mathrm{Im}\ \hat{F}^R, \tag{9}$$

$$\hat{D}^T = (\mathrm{Re}\ \hat{G}^R)^2 + (\mathrm{Im}\ \hat{F}^R)^2, \tag{10}$$

$$\hat{D}^L = (\mathrm{Re}\ \hat{G}^R)^2 - (\mathrm{Re}\ \hat{F}^R)^2. \tag{11}$$

The function $\hat{\Sigma}(\boldsymbol{r},\varepsilon)$ differs from zero only inside the superconductor. It accounts both for energy relaxation of quasiparticles and for their conversion to Cooper pairs due to Andreev reflection. The functions $\hat{D}^T$ and $\hat{D}^L$ acquire space and energy dependencies due to the presence of the superconducting wire and renormalize the diffusion coefficient D.

The solution of Eqs. (7) and (8) can be expressed in terms of the diffusionlike functions $\hat{\mathcal{D}}^T$ and $\hat{\mathcal{D}}^L$ which obey the following equations:

$$-D\,\nabla\,[\hat{D}^T(\boldsymbol{r},\varepsilon)\,\nabla\,\hat{\mathcal{D}}^T(\boldsymbol{r},\boldsymbol{r}',\varepsilon)] + 2\hat{\Sigma}(\boldsymbol{r},\varepsilon)\hat{\mathcal{D}}^T(\boldsymbol{r},\boldsymbol{r}',\varepsilon) = \delta(\boldsymbol{r}-\boldsymbol{r}'), \tag{12}$$

$$-D\,\nabla\,[\hat{D}^L(\boldsymbol{r},\varepsilon)\,\nabla\,\hat{\mathcal{D}}^L(\boldsymbol{r},\boldsymbol{r}',\varepsilon)] = \delta(\boldsymbol{r}-\boldsymbol{r}'). \tag{13}$$

The solutions of Usadel equation (1) in each of the metals should be matched at SF interfaces by means of appropriate boundary conditions which account for electron tunneling between these terminals. The form of these boundary conditions essentially depends on the adopted model describing electron scattering at SF interfaces. Here we stick to the model of the so-called spin-active interfaces[21] which takes into account possibly different barrier transmissions for spin-up and spin-down electrons. This model was already extensively used for theoretical description of different physical phenomena, including spin-resolved CAR in ballistic structures[18,19] and Josephson effect with triplet pairing.[22,23] Here we employ this model in the case of diffusive electrodes and also restrict our analysis to the case of tunnel barriers with channel transmissions much smaller than one. In this case the corresponding boundary conditions read[24]

$$\mathcal{A}\sigma_+\check{G}_+\partial_x\check{G}_+ = \frac{G_T}{2}[\check{G}_-,\check{G}_+] + \frac{G_m}{4}[\{\hat{\boldsymbol{\sigma}}\boldsymbol{m}\tau_3,\check{G}_-\},\check{G}_+] + i\frac{G_\varphi}{2}[\hat{\boldsymbol{\sigma}}\boldsymbol{m}\tau_3,\check{G}_+], \tag{14}$$

$$-\mathcal{A}\sigma_-\check{G}_-\partial_x\check{G}_- = \frac{G_T}{2}[\check{G}_+,\check{G}_-] + \frac{G_m}{4}[\{\hat{\boldsymbol{\sigma}}\boldsymbol{m}\tau_3,\check{G}_+\},\check{G}_-] + i\frac{G_\varphi}{2}[\hat{\boldsymbol{\sigma}}\boldsymbol{m}\tau_3,\check{G}_-], \tag{15}$$

where $\check{G}_-$ and $\check{G}_+$ are the Green-Keldysh functions from the left $(x<0)$ and from the right $(x>0)$ side of the interface, $\mathcal{A}$ is the effective contact area, $\boldsymbol{m}$ is the unit vector in the direction of the interface magnetization, $\sigma_\pm$ are Drude conductivities of the left and right terminals, and G_T is the spin-independent part of the interface conductance. Along with G_T there also exists the spin-sensitive contribution to the interface conductance which is accounted for by the G_m term. The value G_m equals to the difference between interface conductances for spin-up and spin-down conduction bands in the normal state. The G_φ term arises due to different phase shifts acquired by scattered quasiparticles with opposite spin directions.

Employing the above boundary conditions we can establish the following linear relations between the distribution functions at both sides of the interface:

$$\mathcal{A}\sigma_+\hat{D}_+^T\partial_x\hat{f}_{+T} = \mathcal{A}\sigma_-\hat{D}_-^T\partial_x\hat{f}_{-T} = \hat{g}_T(\hat{f}_{+T}-\hat{f}_{-T}) + \hat{g}_m(\hat{f}_{+L}-\hat{f}_{-L}), \tag{16}$$

$$\mathcal{A}\sigma_+\hat{D}_+^L\partial_x\hat{f}_{+L} = \mathcal{A}\sigma_-\hat{D}_-^L\partial_x\hat{f}_{-L} = \hat{g}_L(\hat{f}_{+L}-\hat{f}_{-L}) + \hat{g}_m(\hat{f}_{+T}-\hat{f}_{-T}), \tag{17}$$

where $\hat{g}_T$, $\hat{g}_L$, and $\hat{g}_m$ are matrix interface conductances which depend on the retarded and advanced Green's functions at the interface

$$\hat{g}_T = G_T[(\mathrm{Re}\,\hat{G}_+^R)(\mathrm{Re}\,\hat{G}_-^R) + (\mathrm{Im}\,\hat{F}_+^R)(\mathrm{Im}\,\hat{F}_-^R)], \tag{18}$$

$$\hat{g}_L = G_T[(\mathrm{Re}\,\hat{G}_+^R)(\mathrm{Re}\,\hat{G}_-^R) - (\mathrm{Re}\,\hat{F}_+^R)(\mathrm{Re}\,\hat{F}_-^R)], \tag{19}$$

$$\hat{g}_m = G_m\hat{\boldsymbol{\sigma}}\boldsymbol{m}(\mathrm{Re}\,\hat{G}_+^R)(\mathrm{Re}\,\hat{G}_-^R). \tag{20}$$

Note that the above boundary conditions for the distribution functions do not contain the G_φ term explicitly since this term in Eqs. (14) and (15) does not mix Green's functions from both sides of the interface.

The current density Eq. (5) can then be expressed in terms of the distribution function $\hat{f}_T$ as

$$\boldsymbol{j} = -\frac{\sigma}{4e}\int Sp[\hat{D}^T\nabla\hat{f}_T]d\varepsilon. \tag{21}$$

III. SPECTRAL CONDUCTANCES

Let us now employ the above formalism in order to evaluate electric currents in our FSF device depicted in Fig. 1. The current across the first (SF_1) interface can be written as

$$I_1 = \frac{1}{e}\int g_{11}(\varepsilon)[f_0(\varepsilon+eV_1)-f_0(\varepsilon)]d\varepsilon - \frac{1}{e}\int g_{12}(\varepsilon)[f_0(\varepsilon+eV_2)-f_0(\varepsilon)]d\varepsilon, \tag{22}$$

where $f_0(\varepsilon)=\tanh(\varepsilon/2T)$, g_{11} and g_{12} are local and nonlocal spectral electric conductances. Expression for the current across the second interface can be obtained from the above equation by interchanging the indices $1\leftrightarrow 2$. Solving Eqs. (7) and (8) with boundary conditions in Eqs. (16) and (17) we express both local and nonlocal conductances $\hat{g}_{ij}(\varepsilon)$ in terms of the interface conductances and the function $\hat{\mathcal{D}}$. The corresponding results read

$$\hat{g}_{11}(\varepsilon) = (\hat{R}_2^T\hat{\mathcal{M}}^L + \hat{R}_2^T\hat{R}_2^L\hat{R}_{1m} - \hat{R}_1^L\hat{R}_{2m}^2 + \hat{R}_{12}^T\hat{R}_{12}^L\hat{R}_{2m} - \hat{R}_{1m}\hat{R}_{2m}^2)\hat{\mathcal{K}}, \tag{23}$$

$$\hat{g}_{12}(\varepsilon) = \hat{g}_{21}(\varepsilon) = (\hat{R}_{12}^T\hat{\mathcal{M}}^L + \hat{R}_2^T\hat{R}_{12}^L\hat{R}_{1m} + \hat{R}_{12}^L\hat{R}_{1m}\hat{R}_{2m} + \hat{R}_{12}^T\hat{R}_1^L\hat{R}_{2m})\hat{\mathcal{K}}, \tag{24}$$

where we defined

$$\hat{\mathcal{M}}^{T,L} = \hat{R}_1^{T,L}\hat{R}_2^{T,L} - (\hat{R}_{12}^{T,L})^2, \tag{25}$$

$$\hat{\mathcal{K}}^{-1} = \hat{\mathcal{M}}^T\hat{\mathcal{M}}^L + \hat{R}_{1m}^2\hat{R}_{2m}^2 - \hat{R}_2^T\hat{R}_2^L\hat{R}_{1m}^2 - 2\hat{R}_{12}^T\hat{R}_{12}^L\hat{R}_{1m}\hat{R}_{2m} - \hat{R}_1^T\hat{R}_1^L\hat{R}_{2m}^2 \tag{26}$$

and introduced the auxiliary resistance matrix

$$\hat{R}_1^T = \hat{g}_{1T}(\varepsilon)[\hat{g}_{1T}(\varepsilon)\hat{g}_{1L}(\varepsilon) - \hat{g}_{1m}^2(\varepsilon)]^{-1} + \frac{D_1\hat{\mathcal{D}}_1^T(\boldsymbol{r}_1,\boldsymbol{r}_1,\varepsilon)}{\sigma_1} + \frac{D_S\hat{\mathcal{D}}_S^T(\boldsymbol{r}_1,\boldsymbol{r}_1,\varepsilon)}{\sigma_S}. \tag{27}$$

The resistance matrices $\hat{R}_2^T$, $\hat{R}_1^L$, and $\hat{R}_2^L$ can be obtained by interchanging the indices $1\leftrightarrow 2$ and $T\leftrightarrow L$ in Eq. (27). The remaining resistance matrices $\hat{R}_{12}^{T,L}$ and $\hat{R}_{jm}$ are defined as

$$\hat{R}_{12}^{T,L} = \hat{R}_{21}^{T,L} = \frac{D_S\hat{\mathcal{D}}_S^{T,L}(\boldsymbol{r}_1,\boldsymbol{r}_2,\varepsilon)}{\sigma_S}, \tag{28}$$

$$\hat{R}_{jm} = \hat{g}_{jm}(\varepsilon)[\hat{g}_{jT}(\varepsilon)\hat{g}_{jL}(\varepsilon) - \hat{g}_{jm}^2(\varepsilon)]^{-1}, \tag{29}$$

where $j=1,2$. The spectral conductance g_{ij} can be recovered from the matrix $\hat{g}_{ij}$ simply by summing up over the spin states

$$g_{ij}(\varepsilon) = \frac{1}{2}Sp[\hat{g}_{ij}(\varepsilon)]. \tag{30}$$

It is worth pointing out that Eqs. (23) and (24) defining, respectively, local and nonlocal spectral conductances are presented with excess accuracy. This is because the boundary conditions in Eqs. (14) and (15) employed here remain applicable only in the tunneling limit and for weak spin-dependent scattering $|G_m|,|G_\varphi| \ll G_T$. Hence, strictly speaking only the lowest order terms in $G_{m_{1,2}}$ and $G_{\varphi_{1,2}}$ need to be kept in our final results.

In order to proceed it is necessary to evaluate the interface conductances as well as the matrix functions $\hat{\mathcal{D}}^{T,L}_{1,2,S}$. Restricting ourselves to the second order in the interface transmissions we obtain

$$\hat{g}_{1T}(\varepsilon) = G_{T_1}\hat{\nu}_S(\boldsymbol{r}_1,\varepsilon) + G_{T_1}^2\frac{\Delta^2\theta(\Delta^2-\varepsilon^2)}{\Delta^2-\varepsilon^2}\hat{U}_1(\varepsilon), \tag{31}$$

$$\hat{g}_{1L}(\varepsilon) = G_{T_1}\hat{\nu}_S(\boldsymbol{r}_1,\varepsilon) - G_{T_1}^2\frac{\Delta^2\theta(\varepsilon^2-\Delta^2)}{\varepsilon^2-\Delta^2}\hat{U}_1(\varepsilon), \tag{32}$$

$$\hat{g}_{1m}(\varepsilon) = G_{m_1}\hat{\nu}_S(\boldsymbol{r}_1,\varepsilon)\hat{\boldsymbol{\sigma}}\boldsymbol{m}_1, \tag{33}$$

and analogous expressions for the interface conductances of the second interface. The matrix function

$$\hat{U}_1(\varepsilon) = \frac{D_1}{2\sigma_1}\{\mathrm{Re}[\mathcal{C}_1(\boldsymbol{r}_1,\boldsymbol{r}_1,2h_1^+) + \mathcal{C}_1(\boldsymbol{r}_1,\boldsymbol{r}_1,2h_1^-)] - \hat{\boldsymbol{\sigma}}\boldsymbol{m}_1\,\mathrm{Re}[\mathcal{C}_1(\boldsymbol{r}_1,\boldsymbol{r}_1,2h_1^+) - \mathcal{C}_1(\boldsymbol{r}_1,\boldsymbol{r}_1,2h_1^-)]\} \tag{34}$$

with $h_1^\pm = h_1 \pm \varepsilon$ defines the correction due to the proximity effect in the normal metal.

Taking into account the first-order corrections in the interface transmissions one can derive the density of states inside the superconductor in the following form:

$$\hat{\nu}_S(\boldsymbol{r},\varepsilon) = \frac{|\varepsilon|\theta(\varepsilon^2-\Delta^2)}{\sqrt{|\varepsilon^2-\Delta^2|}} + \frac{D_S}{\sigma_S}\frac{\Delta^2}{\Delta^2-\varepsilon^2}\sum_{i=1,2}[G_{T_i}\,\mathrm{Re}\,\mathcal{C}_S(\boldsymbol{r},\boldsymbol{r}_i,2\omega^R) - \hat{\boldsymbol{\sigma}}\boldsymbol{m}_i G_{\varphi_i}\,\mathrm{Im}\,\mathcal{C}_S(\boldsymbol{r},\boldsymbol{r}_i,2\omega^R)], \tag{35}$$

where

$$\omega^R = \begin{cases} \sqrt{\varepsilon^2-\Delta^2} & \varepsilon > \Delta \\ i\sqrt{\Delta^2-\varepsilon^2} & |\varepsilon| < \Delta \\ -\sqrt{\varepsilon^2-\Delta^2} & \varepsilon < \Delta, \end{cases} \tag{36}$$

and the Cooperon $\mathcal{C}_j(\boldsymbol{r},\boldsymbol{r}',\varepsilon)$ represents the solution of the equation

$$(-D\nabla^2 - i\varepsilon)\mathcal{C}(\boldsymbol{r},\boldsymbol{r}',\varepsilon) = \delta(\boldsymbol{r}-\boldsymbol{r}') \tag{37}$$

in the normal metal leads ($j=1,2$) and the superconductor ($j=S$). In the quasi-one-dimensional geometry the corresponding solutions take the form

$$\mathcal{C}_j(x_j,x_j,\varepsilon) = \frac{\tanh(k_jL_j)}{S_jD_jk_j}, \quad j=1,2, \tag{38}$$

$$\mathcal{C}_S(x,x',\varepsilon) = \frac{\sinh[k_S(L-x')]\sinh k_Sx}{k_SS_SD_S\sinh(k_SL)}, \quad x' > x, \tag{39}$$

where $S_{S,1,2}$ are the wire cross sections and $k_{1,2,S} = \sqrt{-i\varepsilon/D_{1,2,S}}$.

Substituting Eq. (35) into Eqs. (31) and (32) and comparing the terms $\propto G_{T_1}^2$ we observe that the tunneling correction to the density of states dominates over the terms proportional to $\hat{U}_1$ which contain an extra small factor $\sqrt{\Delta/h} \ll 1$. Hence, the latter terms in Eqs. (31) and (32) can be safely neglected. In addition, in Eq. (35) we also neglect small tunneling corrections to the superconducting density of states at energies exceeding the superconducting gap Δ. Within this approximation the density of states inside the superconducting wire becomes spin-independent $\hat{\nu}_S(\boldsymbol{r},\varepsilon) = \hat{\sigma}_0\nu_S(\boldsymbol{r},\varepsilon)$. It can then be written as

$$\nu_S(\boldsymbol{r},\varepsilon) = \frac{|\varepsilon|}{\sqrt{|\varepsilon^2-\Delta^2|}}\theta(\varepsilon^2-\Delta^2) + \frac{D_S}{\sigma_S}\frac{\Delta^2\theta(\Delta^2-\varepsilon^2)}{\Delta^2-\varepsilon^2}\sum_{i=1,2}G_{T_i}\,\mathrm{Re}\,\mathcal{C}_S(\boldsymbol{r},\boldsymbol{r}_i,2\omega^R). \tag{40}$$

Accordingly, the interface conductances take the form

$$\hat{g}_{1T}(\varepsilon) = \hat{g}_{1L}(\varepsilon) = G_{T_1}\nu_S(\boldsymbol{r}_1,\varepsilon), \tag{41}$$

$$\hat{g}_{1m}(\varepsilon) = G_{m_1}\nu_S(\boldsymbol{r}_1,\varepsilon)\hat{\boldsymbol{\sigma}}\boldsymbol{m}_1. \tag{42}$$

Let us emphasize again that within our approximation the G_φ term does not enter into expressions for the interface conductances in Eqs. (41) and (42) and, hence, does not appear in the final expressions for the conductances $g_{ij}(\varepsilon)$.

In the limit of strong exchange fields $h_{1,2} \gg \Delta$ and small interface transmissions considered here the proximity effect in the ferromagnets remains weak and can be neglected. Hence, the functions $\hat{\mathcal{D}}_1^{T,L}(\boldsymbol{r}_1,\boldsymbol{r}_1,\varepsilon)$ and $\hat{\mathcal{D}}_2^{T,L}(\boldsymbol{r}_2,\boldsymbol{r}_2,\varepsilon)$ can be approximated by their normal-state values

$$\hat{\mathcal{D}}_1^{T,L}(\boldsymbol{r}_1,\boldsymbol{r}_1,\varepsilon) = \sigma_1 r_{N_1}\hat{1}/D_1, \tag{43}$$

$$\hat{\mathcal{D}}_2^{T,L}(\boldsymbol{r}_2,\boldsymbol{r}_2,\varepsilon) = \sigma_2 r_{N_2}\hat{1}/D_2, \tag{44}$$

$$r_{N_j} = L_j/(\sigma_jS_j), \quad j=1,2, \tag{45}$$

where r_{N_1} and r_{N_2} are the normal-state resistances of ferromagnetic terminals. In the superconducting region an effective expansion parameter is $G_{T_{1,2}}r_{\xi_S}(\varepsilon)$, where $r_{\xi_S}(\varepsilon) = \xi_S(\varepsilon)/(\sigma_SS_S)$ is the Drude resistance of the superconducting wire segment of length $\xi_S(\varepsilon) = \sqrt{D_S/2|\omega^R|}$ and ω^R is the function of ε according to Eq. (36). In the limit

$$G_{T_{1,2}}r_{\xi_S}(\varepsilon) \ll 1, \tag{46}$$

which is typically well satisfied for realistic system parameters, it suffices to evaluate the function $\hat{\mathcal{D}}_S^T(x,x',\varepsilon)$ for impenetrable interfaces. In this case we find

$$\hat{\mathcal{D}}_S^T(x,x',\varepsilon) = \begin{cases} \dfrac{\Delta^2-\varepsilon^2}{\Delta^2}\mathcal{C}_S(x,x',2\omega^R) & |\varepsilon|<\Delta \\ \dfrac{\varepsilon^2-\Delta^2}{\varepsilon^2}\mathcal{C}_S(x,x',0) & |\varepsilon|>\Delta. \end{cases} \quad (47)$$

We note that special care should be taken while calculating $\mathcal{D}_S^L(x,x',\varepsilon)$ at subgap energies, since the coefficient D^L in Eq. (8) tends to zero deep inside the superconductor. Accordingly, the function $\mathcal{D}_S^L(x,x',\varepsilon)$ becomes singular in this case. Nevertheless, the combinations $\hat{R}_j^L(\mathcal{M}^L)^{-1}$ and $\hat{R}_{12}^L(\mathcal{M}^L)^{-1}$ remain finite also in this limit. At subgap energies we obtain

$$\hat{R}_1^L(\hat{\mathcal{M}}^L)^{-1} = \hat{R}_2^L(\hat{\mathcal{M}}^L)^{-1} = \hat{R}_{12}^L(\hat{\mathcal{M}}^L)^{-1} = \frac{1}{r_{N_1}+r_{N_2}+\dfrac{2(\Delta^2-\varepsilon^2)e^{d/\xi_S(\varepsilon)}}{\Delta^2 r_{\xi_S}(\varepsilon)G_{T_1}G_{T_2}}}, \quad (48)$$

where $d=|x_2-x_1|$ is the distance between two SF contacts. Substituting the above relations into Eq. (24) we arrive at the final result for the nonlocal spectral conductance of our device at subgap energies

$$g_{12}(\varepsilon) = g_{21}(\varepsilon) = \frac{\Delta^2-\varepsilon^2}{\Delta^2}\frac{r_{\xi_S}(\varepsilon)\exp[-d/\xi_S(\varepsilon)]}{2[r_{N_1}+1/g_{T1}(\varepsilon)][r_{N_2}+1/g_{T2}(\varepsilon)]}$$
$$\times\left[1+\boldsymbol{m}_1\boldsymbol{m}_2\frac{G_{m1}}{g_{T1}(\varepsilon)}\frac{G_{m2}}{g_{T2}(\varepsilon)}\frac{\Delta^2}{\Delta^2-\varepsilon^2}\frac{1}{1-\dfrac{\varepsilon^2}{\Delta^2}+\dfrac{r_{N_1}+r_{N_2}}{2}r_{\xi_S}(\varepsilon)G_{T_1}G_{T_2}\exp[-d/\xi_S(\varepsilon)]}\right], \quad |\varepsilon|<\Delta. \quad (49)$$

Equation (49) represents the central result of our paper. It consists of two different contributions. The first of them is independent of the interface polarizations $\boldsymbol{m}_{1,2}$. This term represents direct generalization of the result[17] in two different aspects. Firstly, the analysis[17] was carried out under the assumption $r_{N_{1,2}}g_{T1,2}(\varepsilon)\ll 1$ which is abandoned here. Secondly (and more importantly), sufficiently large exchange fields $h_{1,2}\gg\Delta$ of ferromagnetic electrodes suppress disorder-induced electron interference in these electrodes and, hence, eliminate the corresponding zero-bias anomaly both in local[25–27] and nonlocal[17] spectral conductances. In this case with sufficient accuracy one can set $g_{Ti}(\varepsilon)=G_{Ti}\nu_S(x_i,\varepsilon)$ implying that at subgap energies $g_{Ti}(\varepsilon)$ is entirely determined by the second term in Eq. (40) which yields in the case of quasi-one-dimensional electrodes

$$g_{T1}(\varepsilon) = \frac{\Delta^2 G_{T_1}r_{\xi_S}(\varepsilon)}{2(\Delta^2-\varepsilon^2)}[G_{T_1}+G_{T_2}e^{-d/\xi_S(\varepsilon)}], \quad (50)$$

$$g_{T2}(\varepsilon) = \frac{\Delta^2 G_{T_2}r_{\xi_S}(\varepsilon)}{2(\Delta^2-\varepsilon^2)}[G_{T_2}+G_{T_1}e^{-d/\xi_S(\varepsilon)}]. \quad (51)$$

Note, that if the exchange field $h_{1,2}$ in both normal electrodes is reduced well below Δ and eventually is set equal to zero, the term containing $\hat{U}_1(\varepsilon)$ in Eqs. (31) and (32) becomes important and should be taken into account. In this case we again recover the zero-bias anomaly[25–27] $g_{Ti}(\varepsilon)\propto 1/\sqrt{\varepsilon}$ and from the first term in Eq. (49) we reproduce the results[17] derived in the limit $h_{1,2}\to 0$.

The second term in Eq. (49) is proportional to the product $\boldsymbol{m}_1\boldsymbol{m}_2G_{m1}G_{m2}$ and describes nonlocal magnetoconductance effect in our system emerging due to spin-sensitive electron scattering at SF interfaces. It is important that—despite the strong inequality $|G_{mi}|\ll G_{Ti}$—both terms in Eq. (49) can be of the same order, i.e., the second (magnetic) contribution can significantly modify the nonlocal conductance of our device.

In the limit of large interface resistances $r_{N_{1,2}}g_{T1,2}(\varepsilon)\ll 1$ the formula (49) reduces to a much simpler one

$$g_{12}(\varepsilon) = g_{21}(\varepsilon) = \frac{r_{\xi_S}(\varepsilon)}{2}\exp[-d/\xi_S(\varepsilon)] \times\left[\frac{\Delta^2-\varepsilon^2}{\Delta^2}g_{T1}(\varepsilon)g_{T2}(\varepsilon)+\boldsymbol{m}_1\boldsymbol{m}_2G_{m1}G_{m2}\frac{\Delta^2}{\Delta^2-\varepsilon^2}\right]. \quad (52)$$

Interestingly, Eq. (52) remains applicable for arbitrary values of the angle between interface polarizations $\boldsymbol{m}_1$ and $\boldsymbol{m}_2$ and strongly resembles the analogous result for the nonlocal conductance in ballistic FSF systems [cf., e.g., Eq. (77) in Ref. 18]. The first term in the square brackets in Eq. (52) describes the fourth-order contribution in the interface transmissions which remains nonzero also in the limit of the nonferromagnetic leads.[17] In contrast, the second term is proportional to the product of transmissions of both interfaces, i.e., only to the second order in barrier transmissions.[3,18] This term vanishes identically provided at least one of the interfaces is spin isotropic.

Contrary to the nonlocal conductance at subgap energies, both local conductance (at all energies) and nonlocal spectral conductance at energies above the superconducting gap are only weakly affected by magnetic effects. Neglecting small corrections due to G_m term in the boundary conditions we obtain

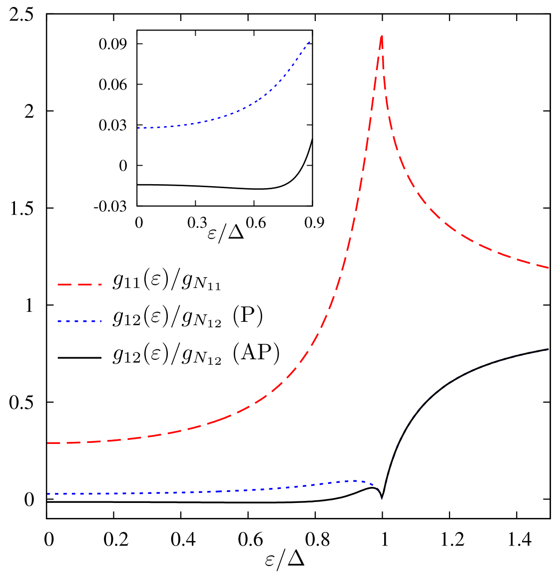

FIG. 2. (Color online) Local (long-dashed line) and nonlocal (short-dashed and solid lines) spectral conductances normalized to its normal-state values. Here we choose $r_{N_1}=r_{N_2}=5r_{\xi_S}(0)$, $x_1=L-x_2=5\xi_S(0)$, $x_2-x_1=\xi_S(0)$ and, $G_{T_1}=G_{T_2}=4G_{m_1}=4G_{m_2}=0.2/r_{\xi_S}(0)$. Energy dependence of nonlocal conductance is displayed for P $\boldsymbol{m}_1\boldsymbol{m}_2=1$ and AP $\boldsymbol{m}_1\boldsymbol{m}_2=-1$ interface magnetizations. Inset: the same in the limit of low energies.

$$\hat{g}_{11}(\varepsilon)=\hat{R}_1^T(\hat{\mathcal{M}}^T)^{-1}, \quad \hat{g}_{22}(\varepsilon)=\hat{R}_2^T(\hat{\mathcal{M}}^T)^{-1}, \tag{53}$$

$$\hat{g}_{12}(\varepsilon)=g_{21}(\varepsilon)=\hat{R}_{12}^T(\hat{\mathcal{M}}^T)^{-1}, \quad |\varepsilon|>\Delta. \tag{54}$$

Equations (53) and (54) together with the above expressions for the nonlocal subgap conductance enable one to recover both local and nonlocal spectral conductances of our system at all energies. Typical energy dependencies for both $g_{11}(\varepsilon)$ and $g_{12}(\varepsilon)$ are displayed in Fig. 2. For instance, we observe that at subgap energies the nonlocal conductance g_{12} changes its sign being positive for parallel (P) and negative for antiparallel (AP) interface polarizations.

Having established the spectral conductance matrix $g_{ij}(\varepsilon)$ one can easily recover the complete *I-V* curves for our hybrid FSF structure. In the limit of low-bias voltages these *I-V* characteristics become linear, i.e.,

$$I_1=G_{11}(T)V_1+G_{12}(T)V_2, \tag{55}$$

$$I_2=G_{21}(T)V_1+G_{22}(T)V_2, \tag{56}$$

where $G_{ij}(T)$ represents the linear conductance matrix defined as

$$G_{ij}(T)=\frac{1}{4T}\int g_{ij}(\varepsilon)\frac{d\varepsilon}{\cosh^2\dfrac{\varepsilon}{2T}}. \tag{57}$$

It may also be convenient to invert the relations in Eqs. (55) and (56) thus expressing induced voltages $V_{1,2}$ in terms of injected currents $I_{1,2}$

$$V_1=R_{11}(T)I_1-R_{12}(T)I_2, \tag{58}$$

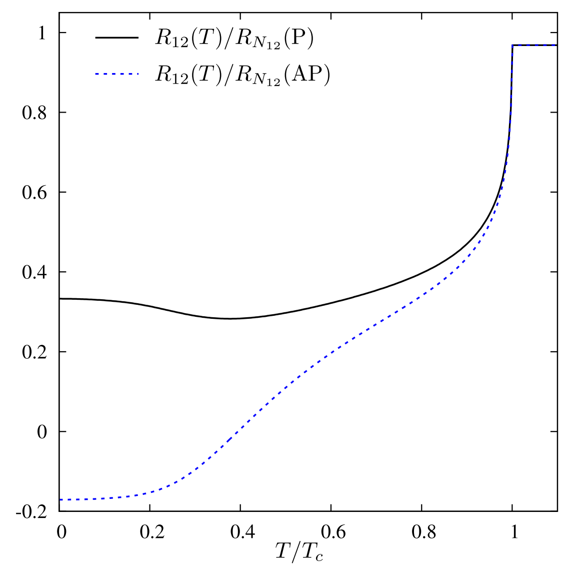

FIG. 3. (Color online) Nonlocal resistance (normalized to its normal-state value) versus temperature (normalized to the superconducting critical temperature T_C) for P and AP interface magnetizations. The parameters are the same as in Fig. 2.

$$V_2=-R_{21}(T)I_1+R_{22}(T)I_2, \tag{59}$$

where the coefficients $R_{ij}(T)$ define local $(i=j)$ and nonlocal $(i\neq j)$ resistances

$$R_{11}(T)=\frac{G_{22}(T)}{G_{11}(T)G_{22}(T)-G_{12}^2(T)}, \tag{60}$$

$$R_{12}(T)=R_{21}(T)=\frac{G_{12}(T)}{G_{11}(T)G_{22}(T)-G_{12}^2(T)} \tag{61}$$

and similarly for $R_{22}(T)$. In nonferromagnetic NSN structures the low-temperature nonlocal resistance $R_{12}(T\to 0)$ turns out to be independent of both the interface conductances and the parameters of the normal leads.[17] However, this universality of R_{12} does not hold anymore provided nonmagnetic normal-metal leads are substituted by ferromagnets. Nonlocal linear resistance R_{12} of our FSF structure is displayed in Figs. 3 and 4 as a function of temperature for parallel $(\boldsymbol{m}_1\boldsymbol{m}_2=1)$ and antiparallel $(\boldsymbol{m}_1\boldsymbol{m}_2=-1)$ interface magnetizations. In Fig. 3 we show typical temperature behavior of the nonlocal resistance for sufficiently transparent interfaces. For both mutual interface magnetizations R_{12} first decreases with temperature below T_C similarly to the nonmagnetic case. However, at lower T important differences occur: while in the case of parallel magnetizations R_{12} always remains positive and even shows a noticeable upturn at sufficiently low T, the nonlocal resistance for antiparallel magnetizations keeps monotonously decreasing with T and may become negative in the low-temperature limit. In the limit of very low interface transmissions the temperature dependence of the nonlocal resistance exhibits a well-pronounced charge imbalance peak (see Fig. 4) whose physics is similar to that analyzed in the case of nonferromagnetic NSN structures.[4,16,23] Let us point out that the above behav-

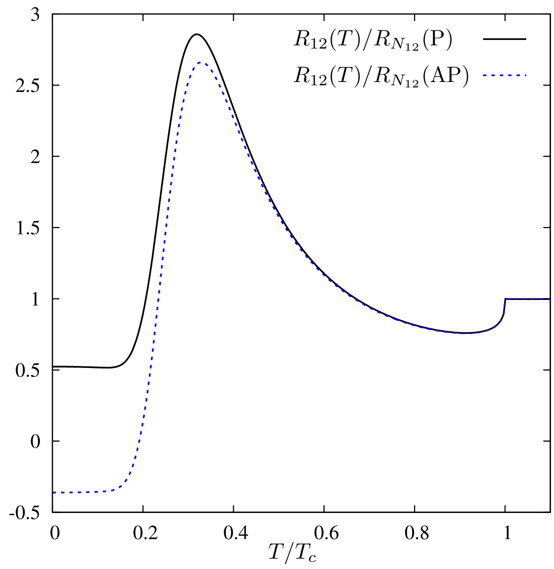

FIG. 4. (Color online) The same as in Fig. 3 for the following parameter values: $r_{N_1}=r_{N_2}=5r_{\xi_S}(0)$, $x_1=L-x_2=5\xi_S(0)$, $x_2-x_1=\xi_S(0)$, and $G_{T_1}=G_{T_2}=50G_{m_1}=50G_{m_2}=0.025/r_{\xi_S}(0)$.

ior of the nonlocal resistance is qualitatively consistent with available experimental observations.[5] More experiments would be desirable in order to quantitatively verify our theoretical predictions.

IV. CONCLUDING REMARKS

In this paper we developed a quantitative theory of nonlocal electron transport in three-terminal hybrid ferromagnet-superconductor-ferromagnet structures in the presence of disorder in the electrodes. Within our model transfer of electrons across SF interfaces is described in the tunneling limit and magnetic properties of the system are accounted for by introducing (i) exchange fields $\boldsymbol{h}_{1,2}$ in both normal-metal electrodes and (ii) magnetizations $\boldsymbol{m}_{1,2}$ of both SF interfaces (the model of spin-active interfaces). The two ingredients (i) and (ii) of our model are, in general, independent of each other and have different physical implications. While the role of (comparatively large) exchange fields $h_{1,2} \gg \Delta$ is merely to suppress disorder-induced interference of electrons[25–27] penetrating from a superconductor into ferromagnetic electrodes, spin-sensitive electron scattering at SF interfaces yields an extra contribution to the nonlocal conductance which essentially depends on relative orientations of the interface magnetizations. For antiparallel magnetizations the total nonlocal conductance g_{12} and resistance R_{12} can turn negative at sufficiently low energies/temperatures. At higher temperatures the difference between the values of R_{12} evaluated for parallel and antiparallel magnetizations becomes less important. At such temperatures the nonlocal resistance behaves similarly to the nonmagnetic case demonstrating, e.g., a well-pronounced charge imbalance peak[17] in the limit of low interface transmissions.

We believe that our predictions can be directly used for quantitative analysis of future experiments on nonlocal electron transport in hybrid FSF structures.

ACKNOWLEDGMENTS

This work was supported in part by DFG and RFBR under Grant No. 09-02-00886. M.S.K. also acknowledges support from the Council for grants of the Russian President (Grant No. 89.2009.2) and from the Dynasty Foundation.

[1] A. F. Andreev, Sov. Phys. JETP **19**, 1228 (1964).
[2] J. M. Byers and M. E. Flatte, Phys. Rev. Lett. **74**, 306 (1995); G. Deutscher and D. Feinberg, Appl. Phys. Lett. **76**, 487 (2000).
[3] G. Falci, D. Feinberg, and F. W. J. Hekking, EPL **54**, 255 (2001).
[4] M. S. Kalenkov and A. D. Zaikin, Phys. Rev. B **75**, 172503 (2007); JETP Lett. **87**, 140 (2008).
[5] D. Beckmann, H. B. Weber, and H. v. Löhneysen, Phys. Rev. Lett. **93**, 197003 (2004).
[6] S. Russo, M. Kroug, T. M. Klapwijk, and A. F. Morpurgo, Phys. Rev. Lett. **95**, 027002 (2005).
[7] P. Cadden-Zimansky and V. Chandrasekhar, Phys. Rev. Lett. **97**, 237003 (2006); P. Cadden-Zimansky, Z. Jiang, and V. Chandrasekhar, New J. Phys. **9**, 116 (2007).
[8] A. Kleine, A. Baumgartner, J. Trbovic, and C. Schönenberger, EPL **87**, 27011 (2009); A. Kleine, A. Baumgartner, J. Trbovic, D. S. Golubev, A. D. Zaikin, and C. Schönenberger, Nanotechnology **21**, 274002 (2010).
[9] B. Almog, S. Hacohen-Gourgy, A. Tsukernik, and G. Deutscher, Phys. Rev. B **80**, 220512(R) (2009).
[10] J. Brauer, F. Hübler, M. Smetanin, D. Beckmann, and H. v. Löhneysen, Phys. Rev. B **81**, 024515 (2010).
[11] A. Levy Yeyati, F. S. Bergeret, A. Martin-Rodero, and T. M. Klapwijk, Nat. Phys. **3**, 455 (2007).
[12] D. S. Golubev and A. D. Zaikin, EPL **86**, 37009 (2009).
[13] A. Brinkman and A. A. Golubov, Phys. Rev. B **74**, 214512 (2006).
[14] J. P. Morten, A. Brataas, and W. Belzig, Phys. Rev. B **74**, 214510 (2006).
[15] R. Mélin, Phys. Rev. B **73**, 174512 (2006).
[16] D. S. Golubev and A. D. Zaikin, Phys. Rev. B **76**, 184510 (2007).
[17] D. S. Golubev, M. S. Kalenkov, and A. D. Zaikin, Phys. Rev. Lett. **103**, 067006 (2009).
[18] M. S. Kalenkov and A. D. Zaikin, Phys. Rev. B **76**, 224506 (2007).
[19] M. S. Kalenkov and A. D. Zaikin, Physica E **40**, 147 (2007).
[20] See, e.g., W. Belzig, F. Wilhelm, C. Bruder, G. Schön, and A. D. Zaikin, Superlattices Microstruct. **25**, 1251 (1999).
[21] M. Eschrig, Phys. Rev. B **80**, 134511 (2009).
[22] M. Eschrig, J. Kopu, J. C. Cuevas, and G. Schön, Phys. Rev. Lett. **90**, 137003 (2003); M. Eschrig and T. Lofwander, Nat. Phys. **4**, 138 (2008).
[23] A. V. Galaktionov, M. S. Kalenkov, and A. D. Zaikin, Phys. Rev. B **77**, 094520 (2008); M. S. Kalenkov, A. V. Galaktionov, and A. D. Zaikin, *ibid.* **79**, 014521 (2009).

[24] D. Huertas-Hernando, Yu. V. Nazarov, and W. Belzig, Phys. Rev. Lett. **88**, 047003 (2002); A. Cottet, D. Huertas-Hernando, W. Belzig, and Yu. V. Nazarov, Phys. Rev. B **80**, 184511 (2009).
[25] A. F. Volkov, A. V. Zaitsev, and T. M. Klapwijk, Physica C **210**, 21 (1993).
[26] F. W. J. Hekking and Yu. V. Nazarov, Phys. Rev. Lett. **71**, 1625 (1993).
[27] A. D. Zaikin, Physica B **203**, 255 (1994).